Indian J. Met. Hydrol. Geophys. (1978), **29**, 1 & 2, 5-15

551.513 : 551.553.21 (5-12)

Cross-equatorial flow over southeast Asia during the northeast monsoon

JOO TICK LIM and LEONG CHUAN QUAH

Malaysian Meteorological Service, Kuala Lumpur

ABSTRACT. Computations of equatorial trajectories involving the vorticity equation as suggested by Fujita *et al.* (1969) were performed. Comparison of the trajectories for the early and late northeast monsoon months reveals that substantial cross-equatorial flow during the late monsoon period is the result of changes that take place in the Asia monsoon circulation. The causes of the cross-equatorial drift flow are also attributed to these changes with a further requirement of the strengthening of the winds over Southeast Asia especially over area north of latitude 10°N.

1. Introduction

Climatological studies on the northeast monsoon (*e.g.*, Lim 1976) have led to the realization that the northeast monsoon over Southeast Asia to south of 10°N, could be subdivided and treated as two separate periods, namely, the early northeast monsoon and the late northeast monsoon. The early monsoon which begins in November and ends in mid-January, is characterized by the daily presence of the active northern low-level equatorial trough which oscillates within a zone between latitude 10°N and the equator. Heavy rain spells over the Malaysian region during this period can normally be related to the monsoon surges which intensify the equatorial trough and its associated vortices. In contrast, the late monsoon (late January to end of February) is marked by frequent substantial lower tropospheric cross-equatorial flow and to some extent, by the presence of the mid-tropospheric trough (Gan 1968) which extends further south than 10°N. These two synoptic phenomena are attributed as the cause of the drastic "drying out" of the atmosphere north of the equator.

Since the occurrence of the severe drought in Peninsular Malaysia during the 1975-76 monsoon, attention has been directed to the study of the much neglected late monsoon. In particular, the cross-equatorial flow phenomenon of this period attracts the utmost interest. In this paper, some features of the cross-equatorial flow phenomenon are examined through the analysis and comparison of the computed trajectories of air particles over the Southeast Asian region.

2. Methods of computing equatorial trajectories

The earliest studies on trajectories of cross-equatorial flow date back to the work of Cressman (1948) who, based on the assumption of constant absolute vorticity, computed the constant absolute vorticity trajectories. Slightly over a decade later, Johnson and Mörth (1960) applied particle dynamics to determine the cross-equatorial drift trajectories (Fig. 1) over equatorial Africa. They applied the following equations,

$$\frac{du}{dt} - fv = -\frac{1}{\rho}\frac{\partial P}{\partial x} - ku \qquad (1a)$$

$$\frac{dv}{dt} + fu = -\frac{1}{\rho}\frac{\partial P}{\partial y} - kv \qquad (1b)$$

with frictional constant $k = 0$.

Later, Gordon and Taylor (1966), using the same equations with $k = 2{\cdot}5 \times 10^{-5}$ sec^{-1}, carried out computations on trajectories over the Indian Ocean. Though the equations in this instance are more complex, the desired results were obtained.

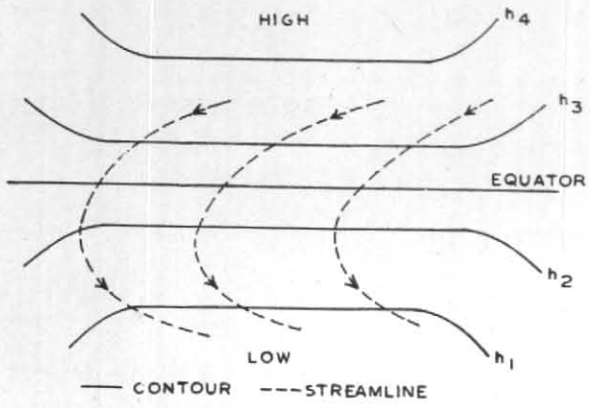

Fig. 1. Schematic pressure distribution and flow pattern associated with the cross-equatorial drift (After Johnson and Morth 1960)

However in both the cases mentioned, the solution of Eqns. (1a) and (1b) were greatly helped by the observation that the pressure field over equatorial Africa and the Indian Ocean is relatively simple and consists of isobars almost parallel to the equator (*see* Fig. 1).

In a more recent work, Fujita *et al.* (1969) performed calculations on cross-equatorial trajectories over the Pacific Ocean based on the vorticity equation which they assumed to be of the form given by Eqn. (2) in the Appendix 1. The use of the vorticity equation avoids the involvement of the pressure element in the computation. This is important as pressure distribution over equatorial regions other than equatorial Africa or the Indian Ocean, could be more complex, thus rendering Eqns. (1a) and (1b) intractable.

The pressure field over Southeast Asia during the northeast monsoon is far from simple. As such the computational procedure as suggested by Fujita *et al.* (full details are given in the Appendix 1) would be followed in the present study.

3. The mean gradient level flow during the northeast monsoon

In the present section and the following five sections, the preparation of the data essential for the trajectory computations will be discussed.

It was decided in the present study to make use of the winds estimated from monthly mean flow charts. This step was taken in view of the sparseness of the present network of upper-air stations in this region. As a result, the analysis of day-to-day flow pattern especially over the sea is still far from accurate.

Figs. 2(a) to 2(d) show mean gradient-level flow charts for the four northeast monsoon months (November to February) compiled by Atkinson and Sadler (1970). Some significant differences in the early monsoon (Figs. 2a and 2b) and the late monsoon flow patterns (Figs. 2c and 2d) are evident. The changes in the late monsoon flow were explained by Sadler and Harris (1970) as due to migrating anticyclones which move eastwards away from China near latitude 25°N. Consequently, the direction of the monsoon acquire a more easterly component. The strong wind belt along the South China coast is also replaced by lighter easterlies and southeasterlies. Over the Malaysian region, the northern equatorial trough which is approximately along latitude 4°N in November, has shifted southwards and lies along latitude 1°N.

4. Divergence and relative vorticity fields

Winds at each $2° \times 2°$ grid point were estimated from the mean flow charts (Figs. 2a—2d). The grid points are located between latitudes 24°N and 14°S and longitudes 90°E and 138°E. The estimated winds were used to compute the divergence (D) and relative vorticity (J) values at the grid points.

Figs. 3 and 4 show an example of each of the computed divergence and the relative vorticity fields. Some interesting features are noted in the D and J patterns of February. As shown in Figs. 3 and 4, the region between 5°N and the equator is an area of divergence and cyclonicity (positive J) while the region between the equator and 8°S is an area of convergence and anticyclonicity (negative J). These patterns are similar to what were observed over the Indian Ocean or equatorial Africa where there are frequent occurrences of cross-equatorial drift flow during the northern winter season.

5. Relationship between divergence and relative vorticity

Fig. 5 shows a scatter diagram with J as the ordinate and D, the abscissa. The scatter diagram was prepared by plotting the grid-point values of J and D located in the area bounded by latitude 20°N and the equator, and longitudes 95°E and 138°E. To reduce the effect of land mass, especially that of Indo China, grid point values of J and D

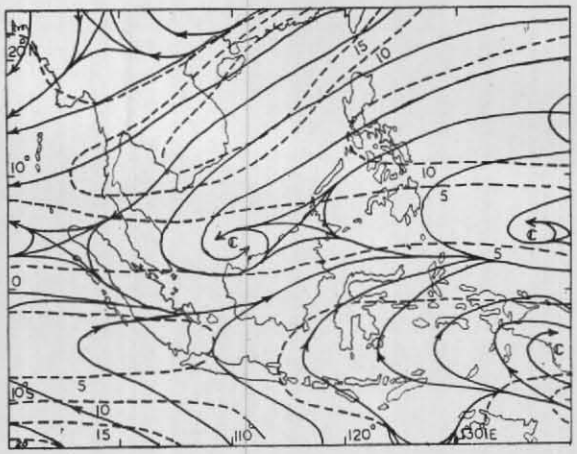

Fig. 2 (a). November

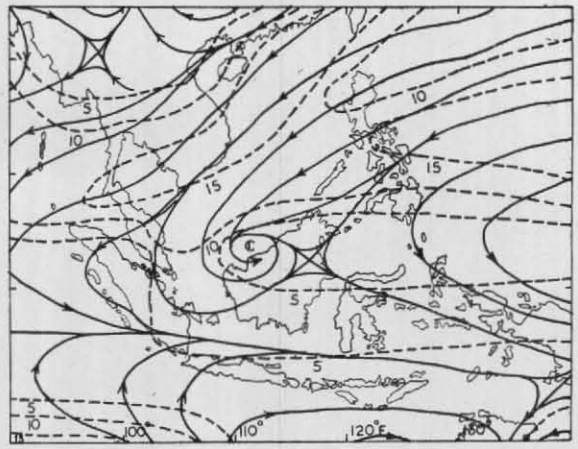

Fig. 2 (b). December

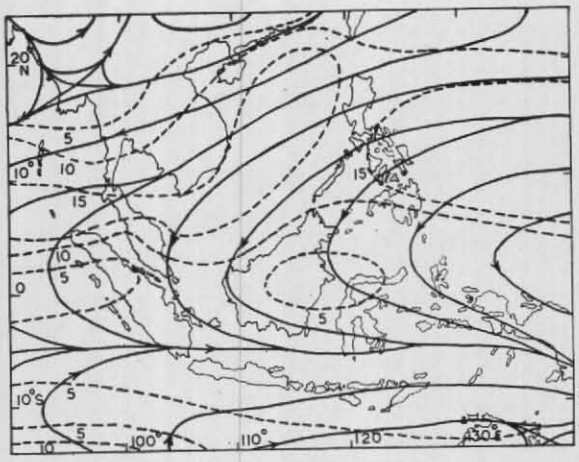

Fig. 2 (c). January

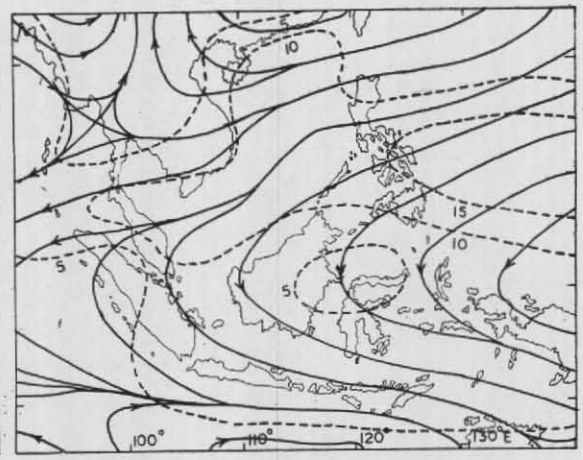

Fig. 2 (d). February

Fig. 2. Resultant gradient-level streamlines and isotach fields (Atkinson 1970)

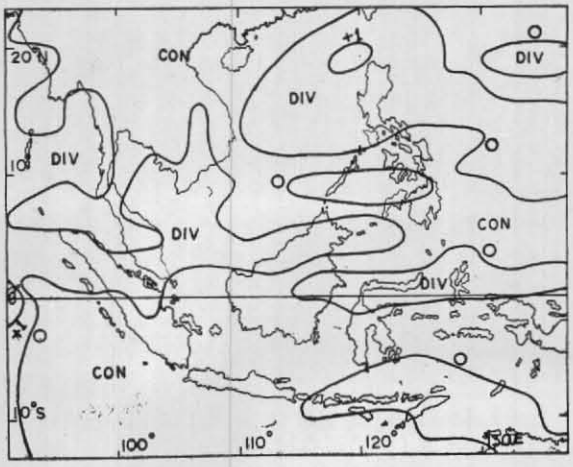

Fig. 3. Divergence (units of 10^{-5} sec^{-1})

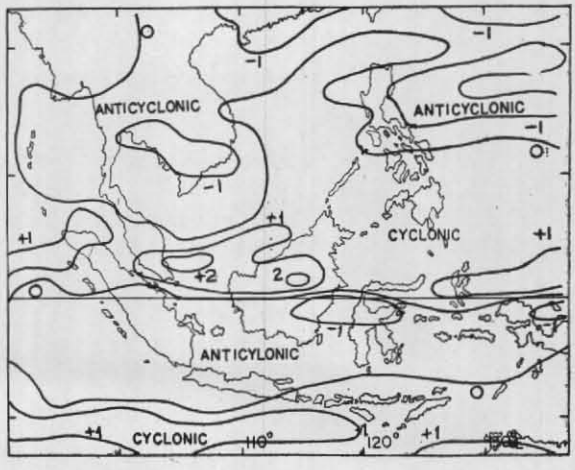

Fig. 4. Relative vorticity (units of 10^{-5} sec^{-1})

Figs. 3 & 4. Mean gradient-level flow for February

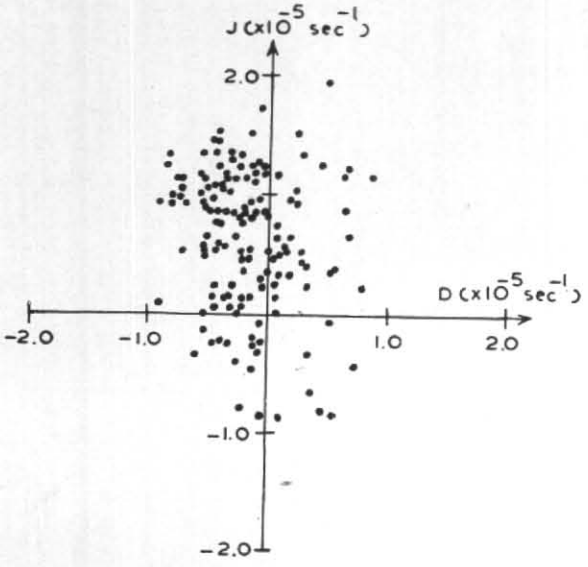

Fig. 5. A scatter diagram of relative vorticity (J) *vs* divergence (D) for November

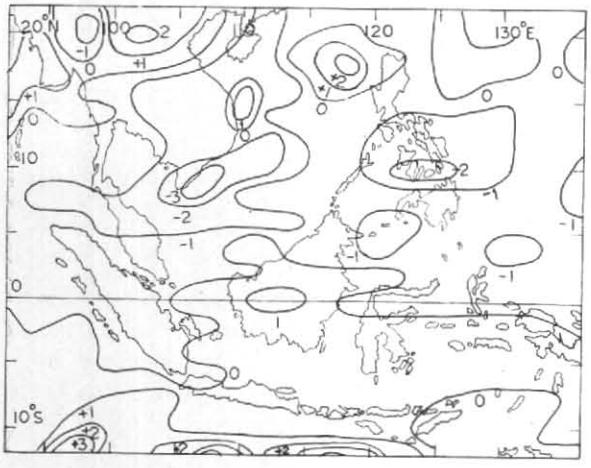

Fig. 6. Rot F (units of 10^{-10} sec^{-2}) field for November

located north of 10°N and east of 110°E were disregarded.

In general, the scatter diagram for each of the four months show fairly large scatter, although there is a tendency for most of the points to clutter either in the upper left or the lower right quadrant. This high degree of scatter is to be expected as the range, between $2{\cdot}0\times10^{-5}$ sec^{-1} and $-2{\cdot}0\times10^{-5}$ sec^{-1} of D and J plotted, is rather small. Within this range, Fig. 7 in the paper by Fujita *et al.* also shows the same degree of scatter.

In this study, it was decided to use all the D and J values of the four monsoon months to determine the approximate linear equation relating

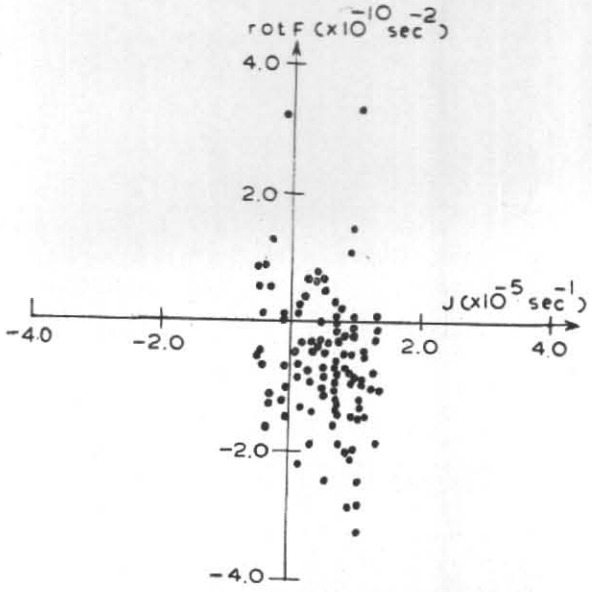

Fig. 7. A scatter diagram of rot F *vs* relative vorticity (J) for November

D and J. This linear equation would then hold for any of the four monsoon months. To proceed, the linear equation was assumed to be :

$$D = AJ$$

A was then evaluated by the least square method and was found to be —0·19. From the empirical relationship, $D = cfJ$, where c is a constant and f is the coriolis parameter at 10°N, we have,

$$c = \frac{A}{f} = 0{\cdot}08\times10^{+5} \text{ sec.}$$

This c-value obtained does not differ very much from that estimated by Fujita *et al.* (1969) for the Pacific Ocean.

6. The absolute vorticity and the vorticity producing force

The absolute vorticity (Q) field was obtained by adding the coriolis parameter to the relative vorticity at each grid point. Knowing the absolute vorticity, divergence and wind fields, the vorticity producing force field (rot F) as shown in Fig. 6 could then be evaluated using the Eqn. (4) in the Appendix 1.

7. Estimation of the frictional constant k

Scatter diagram with J plotted against rot F was prepared for each of the monsoon months using grid-points located in the area north of the

equator and east of Indo China as mentioned in section 5. These diagrams (*e.g.*, Fig. 7) show slightly less scatter than what has been observed in the *J vs D* diagrams. Rot *F* is related to *J* as follows :

$$\text{rot } F = -kJ$$

where k is the frictional constant.

As in the determination of *A*, k is also evaluated using the method of least squares. Since the grid point values of *J* and rot *F* used for the estimation are located mainly over the seas, namely, the South China Sea and the Western Pacific Ocean, k is actually the frictional constant over the seas.

Table 1 shows the value of k for each of the four monsoon months. These k values are relatively low as compared with the value obtained over the Indian Ocean ($k=2{\cdot}5\times10^{-5}$ sec^{-1}) and over the Pacific Ocean ($k=3{\cdot}0\times10^{-5}$ sec^{-1}). The low values obtained for k may be attributed to the mean wind data used for the calculation of the rot *F* and *J* values. Reduction of frictional effect could be expected from mean wind flow as compared with instantaneous flow in case studies carried out by Fujita *et al.* (1969). Errors in estimating k could also be due to the wide scatter of rot *F vs J* diagrams.

TABLE 1

Values of frictional constant (k) for the northeast monsoon months over Southeast Asia

	Frictional constant k
November	$1{\cdot}20\times10^{-5}$ sec^{-1}
December	$1{\cdot}54\times10^{-5}$ „
January	$1{\cdot}05\times10^{-5}$ „
February	$0{\cdot}90\times10^{-5}$ „

To obtain value of k that are more appropriate over the Southeast Asian region, it was therefore decided to use a different but less convincing method of evaluating k. This will be discussed in section 9.

8. Initial values for the trajectories

In this investigation, the trajectories were computed between 15°N and 15°S. Since any air particle reaching the Malaysian-Indonesian region could be traced back to the region around the Philippines bounded by latitudes 10°N and 20°N, and longitudes 110°E and 130°E, the released point was assumed to be 15°N, 120°E. The initial values of speed, direction and relative vorticity of the air were assumed to be the average of the grid point values of these quantities within the "released area" just mentioned.

Table 2 gives the initial conditions for the trajectories for each of the monsoon months. The changes in the monsoon circulation from November through February are reflected in these initial values which are actually the general characteristics of the area around Philippines.

TABLE 2

The initial values for the trajectories.

	Nov	Dec	Jan	Feb
Wind velocity ($\theta°/V$ knots)	060/12	060/14	070/16	070/15
Relative vorticity, J ($\times10^{-5}$ sec^{-1})	0·31	0·18	0·10	—0·12

9. The computation of the trajectories and results

Trajectories for November and February were computed. Trajectories for December and January could be easily deduced from these computed results. The details of the computation procedure are given in the Appendix 1. The time step ($\triangle t$) assumed here was 1 hour.

In the first series of computation, the paths of the air particle were calculated using the initial values as given in Table 2 but varying the k values as follows : $k=0$, 1, 2 and 3 ($\times10^{-5}$ sec^{-1}). Figs. 8(a) and 8(b) show the results of these computations. They reveal that in both the November and February case, the trajectory which agreed most to the mean flow corresponds to $k=2{\cdot}0\times10^{-5}$ sec^{-1}. Therefore, it is probable that k is about $2{\cdot}0\times10^{-5}$ sec^{-1} over the region south of 15°N for whole monsoon period. This inference is considered reasonable because (1) the sea temperatures observed over the seas south of 15°N show no appreciable difference (*cf.* Figs. 9a and 9b) and therefore there should be no change in the k value for the early and late monsoon and (2) this deduced value is nearer to that estimated over the Indian Ocean or the Pacific Ocean.

In the next series of trajectories, the wind speed was allowed to change from 10 to 20, 30, 40 kt and k was assumed to be $2{\cdot}0\times10^{-5}$ sec^{-1}. Comparison of Figs. 10(a) and 10(b) shows that with the same initial wind speed, cross-equatorial flow

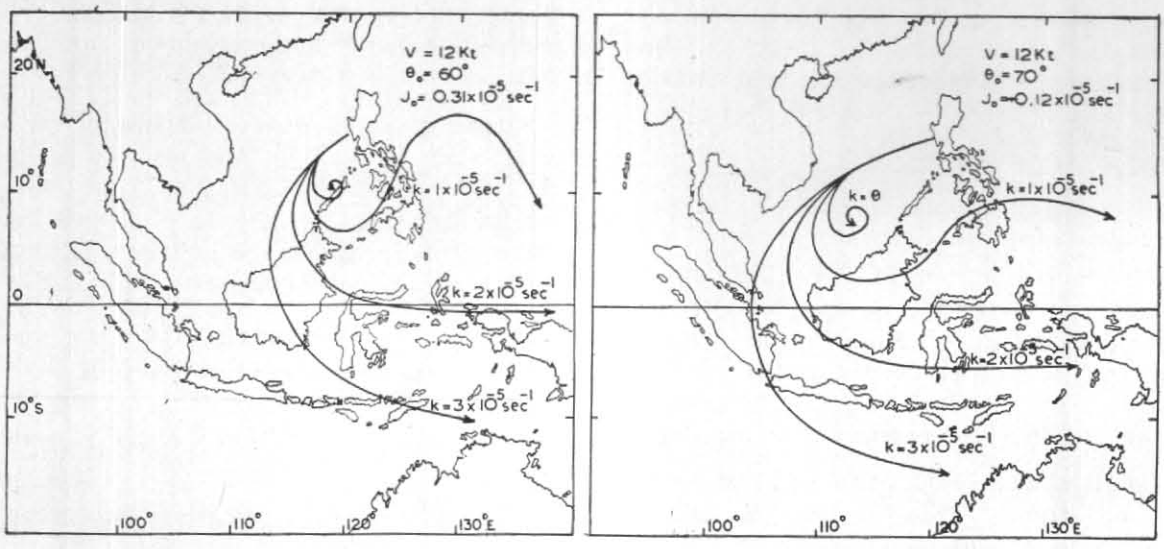

Fig. 8 (a). November

Fig. 8 (b). February

Equatorial trajectories computed for various frictional constants (k)

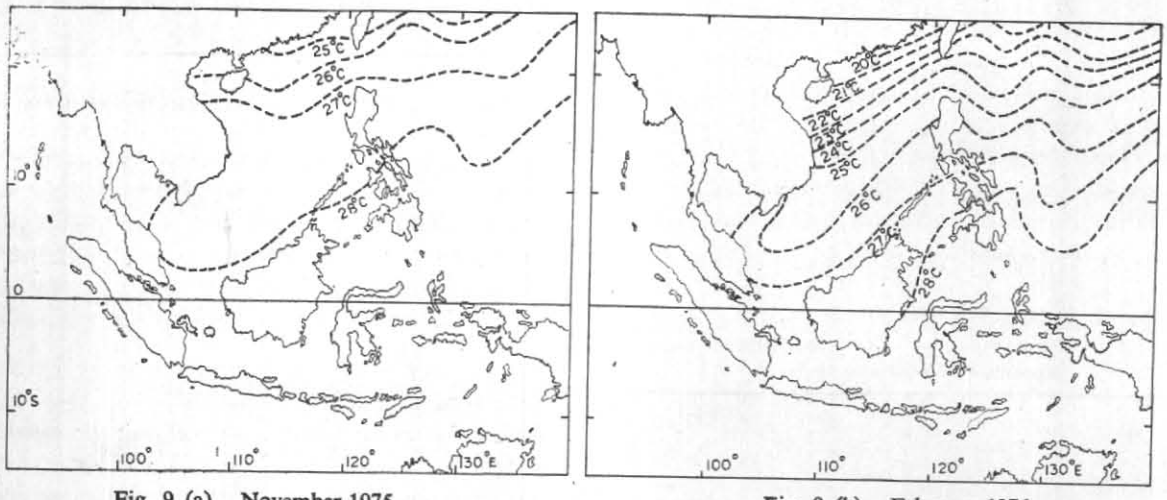

Fig. 9 (a). November 1975

Fig. 9 (b). February 1976

Mean sea-surface temperatures over South China Sea and the Western Pacific Ocean

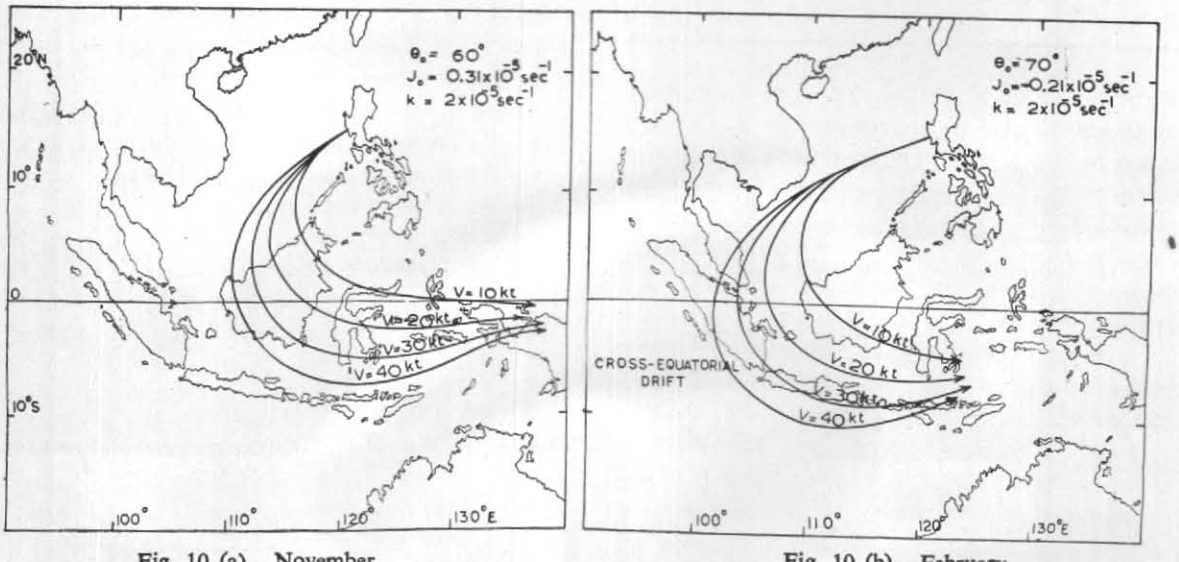

Fig. 10 (a). November

Fig. 10 (b). February

Equatorial trajectories computed for various initial velocities (V)

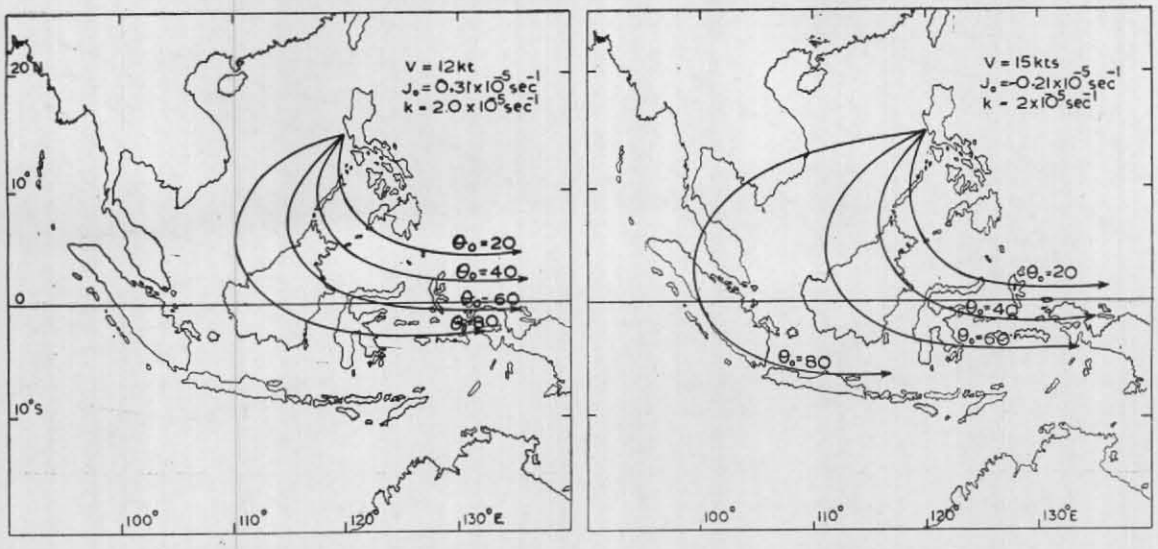

Fig. 11 (a). November

Fig. 11 (b). February

Equatorial trajectories computed for various initial directions (θ_o)

are more likely to occur in February rather than in November. Though the direction of the trajectories in November has a more northerly component, they tend to recurve from the northeasterly to the northwesterly direction very much in the northern hemisphere. In February, the cross-equatorial drift is obtained when the wind speed is increased to 40 kt.

For the final series of computation, the direction (θ) of the air particle at the release point was allowed to change from 010° to 040°, 060° and 080°. In both the November and February months, results (*see* Figs. 11a and 11b) indicate that more cross-equatorial flow can be achieved if the initial direction of the air particle has a more easterly component.

Thus the above analysis of the trajectories show that k can be considered almost constant ($2{\cdot}0 \times 10^{-5}$ sec^{-1}) over the region south of 15°N throughout the northeast monsoon season. Therefore, changes in k are not significant and therefore are not important in determining the cross-equatorial flow phenomenon. However, analysis show that conditions which prevail over the area around Philippines in the late monsoon period, favour cross-equatorial flow over the Malaysian-Indonesian region. These conditions, increase in the easterly component of the winds and anticyclonic vorticity, have been brought about by the changes that have taken place in the low level circulation pattern in East Asia. The cause of the cross-equatorial drift flow during the late monsoon could be attributed to the above mentioned so-called favourable conditions *plus* an increase in the average wind speed over the Philippines region. It must be noted that there are frequent large changes of wind speed (from a monsoon lull of about 5 kt to a monsoon surge of over 40 kt) during the northeast monsoon period and therefore, wind speed variation is an important parameter in modifying the trajectories.

10. A case of cross-equatorial drift flow

Figs. 12(a)—12(f) are shown here to illustrate the occurrence of a gradient level drift flow in January 1976. Surface winds reported by ships were also plotted to augment the poor coverage of the land-based observations. According to Atkinson and Sadler (1970), a good estimate of the gradient level wind could be obtained by increasing the ship wind by 30 to 40 per cent and veering the wind direction by 10 degree if the ship lies in the region north of 5°N.

From 18 through 23 January, there was strengthening of the winds over the seas north of 15°N to an average of about 40 kt (estimated). There was also a slight detectable change in the winds to a more easterly direction. Near the equator, the wind speed also increased corresponding to the speed increase to the north. The weak northern equatorial trough which was present from 18 through 22 January, disappeared on the 23 January

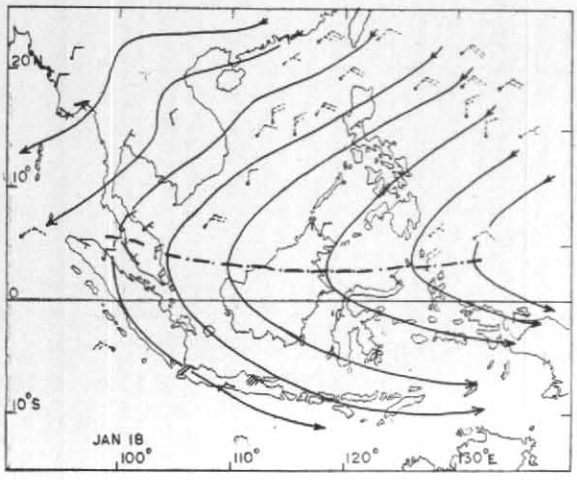

Fig. 12 (a). 18 January 1976

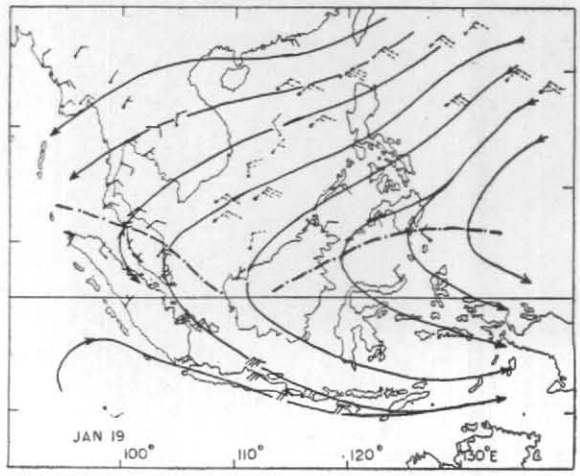

Fig. 12 (b). 19 January 1976

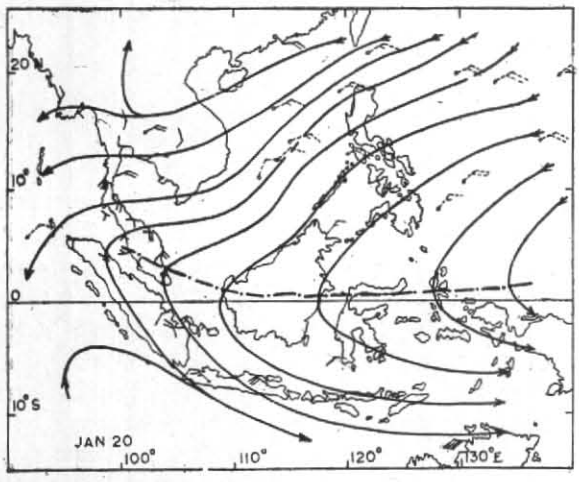

Fig. 12 (c). 20 January 1976

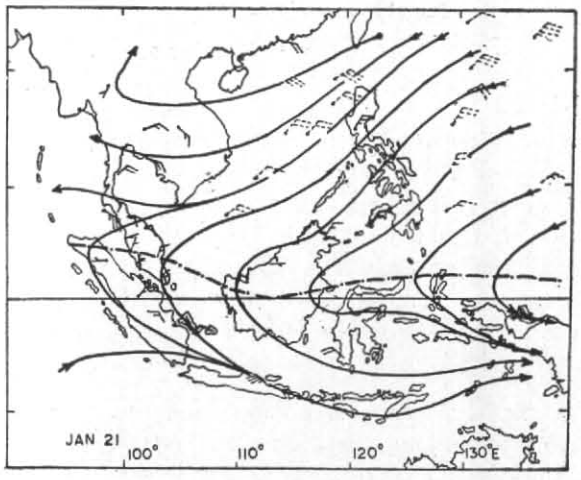

Fig. 12 (d). 21 January 1976

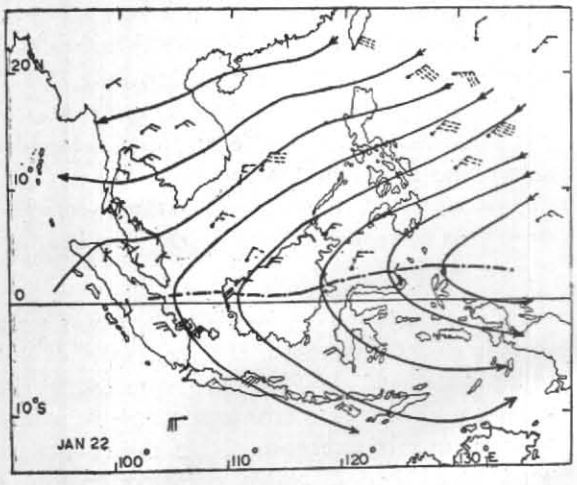

Fig. 12 (e). 22 January 1976

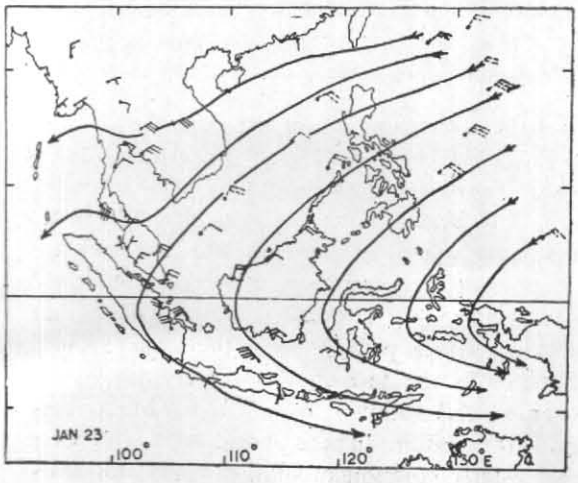

Fig. 12 (f). 23 January 1976

Fig. 12 (a-f). Gradient-level streamlines for 0000 GMT
(Broken arrows denote surface winds reported by ships and dot-dashed line indicates equatorial trough)

and simultaneously, the drift flow made its appearance over Southeast Aisa.

11. Conclusions

Some important features of the cross-equatorial flow over Southeast Asia during the northeast monsoon have been studied through the analysis of the computed equatorial trajectories. It is learnt that certain conditions, specifically, the increase in the easterly component in the winds and the anticyclonic vorticity over the area around Philippines, favour the occurrence of cross-equatorial flow. These conditions have been brought about by the changes that have taken place in the late monsoon circulation. It has been shown that under normal late monsoon conditions, strengthening of the winds over Southeast Asia could produce the cross-equatorial drift phenomenon. The increase in the wind speed could probably be caused by the intensification of the migrating anticyclones north of Philippines.

Acknowledgements

The authors would like to thank the Director-General of Malaysian Meteorological Service for his encouragement and his kind permission to present this paper in the symposium. They are also grateful to Dr. James Pakiam of the University of Singapore, for suggesting improvements to the original draft of this paper.

REFERENCES

Atkinson, G. D. and Sadler, J. C. 1970 Mean-cloudiness and gradient-level wind charts over the tropics. Air weather service (MAC), USAF, Rep. 215.

Cressman, G. C. 1948 Studies of upper-air conditions in low latitudes. Dept. of Met., Univ. of Chicago, Misc. Rep. 24, Pt. 2, pp. 67-103.

Fujita, T. T., Wantanobe, K. and Izawa, T. 1969 *J. appl. Met.*, **8**, pp. 649-667.

Gan, T. L. 1968 The circulation pattern over Singapore and the east coast of West Malaysia during January and February 1967 compared with that of January and February 1968. W.M.O. Training Seminar, Forecasting of heavy rain and floods, Kuala Lumpur, Malaysia, pp. 283-289.

Grodon, A. H. and Taylor, R. C. 1970 Numerical steady-state friction layer trajectories over the oceanic tropics as related to weather. Int. Indian Ocean Expedition, Met. Monogr. 7.

Johnson, D. H. and Morth, H. T. 1960 Forecasting research in East Africa, Tropical Meteorology in Africa (D.J. Bargman Ed.), pp. 56-137. Munitalp Foundation, Nairobi.

Lim, J. T. 1976 *Mon. Weath. Rev.*, **104**, pp. 96-99.

Sadler, C. S. and Harris, B. E. 1970 The mean tropospheric circulation and cloudiness over Southeast Asia and neighbouring areas. Hawaii Inst. Geophys. Sci. Rep. No. 1.

APPENDIX 1

The computation procedures as described below were originated by Fujita *et al.* (1969). The vorticity equation assumed is of the form

$$dQ/dt = -QD + \text{rot}\, \underset{\sim}{F} \tag{2}$$

where $\underset{\sim}{F}$ is the frictional force; Q the absolute vorticity, D the divergence and rot the rotation of a vector.

Introducing friction in a linear form in (2) gives

$$dQ/dt = -QD - \text{rot}\ k\ \underset{\sim}{V}$$

$$= -QD - kJ \tag{3}$$

where k is the frictional constant, $\underset{\sim}{V}$ the wind velocity, J the relative vorticity, and $-kJ$ the vorticity dissipating force. In steady state condition,

$$\underset{\sim}{V} \cdot \nabla Q = -QD - kJ$$

$$\underset{\sim}{V} \cdot \nabla (f + J) + (f + J)\, D + kJ = 0 \tag{4}$$

Expressing Eqn. (4) in natural co-ordinates gives

$$V \frac{\partial}{\partial s} (f + J) + (f + J)\, D + kJ = 0 \tag{5}$$

To obtain the difference equation, the following relations are used :

$$V \triangle t = \triangle S$$

and $$\triangle f = \beta \triangle y = \beta V \sin \alpha \triangle t$$

where β is the Rossby parameter and $\alpha = 270 - \theta$ measured counter clockwise from local east

Eqn. (5) thus becomes $\triangle J/\triangle t = -(\beta V \sin \alpha + fD + JD + kJ)$ (6)

From scatter diagram of D *vs* J, it is possible to obtain an approximate linear relationship between D and J in the form

$$D = -AJ \quad \text{where } A \text{ is a positive constant.} \tag{7}$$

A more generalized relationship between D and J can be written as

$$D = -cfJ \quad \text{where } c \text{ is a constant}$$

Then c can be evaluated as follows :

$$c = \frac{A}{\text{a mean value of } f \text{ over the region considered}}$$

Putting Eqn. (7) into Eqn. (6), we have

$$\triangle f/\triangle t = cfJ^2 + (cf^2 - k)\, J - \beta V \sin \alpha \tag{8}$$

Further assumptions are required to solve Eqn. (8). Therefore, if V the wind speed is assumed constant and the lateral wind shear $\partial V/\partial n$ is zero, then we can write $J = V/r$, where r is the radius of curvature of the flow.

The displacements $\triangle x$ and $\triangle y$ of the air particle are then given by

$$\triangle x_n = V \triangle t \cos \alpha_n$$

$$\triangle y_n = V \triangle t \sin \alpha_n$$

and changes in α by

$$\alpha_{n+1} - \alpha_n = \frac{V \triangle t}{r_n} = J_n \triangle t \quad \text{where } n = 0, 1, 2, \ldots \text{p.}$$

DISCUSSION

(Paper presented by Leong Chuan Quah)

PETER J. WEBSTER : Will you please comment upon the spatial coincidence of cyclonic relative vorticity and divergence in the South China Sea at the gradient level and the physical interpretation of such coincidence?

AUTHOR : The chart that I had shown was for February case. If you look at the February mean gradient level chart, the South China Sea is the region of streamline divergence and cyclonic curvature. On the whole over equatorial region, divergence and vorticity do not possess good correlation and in fact this is revealed by the large degree of scatter in the divergence and vorticity diagram.

T. MURAKAMI : Over the South China Sea the largest contribution to vorticity appears to be due to shear effect. Yet this shear effect has been omitted. I think that due to this omission the computed trajectory is directed eastward immediately after the starting point.

AUTHOR : In this study the shear term in vorticity was neglected, otherwise computations would be very difficult. I feel that this is justifiable since we make use of the mean charts rather than the actual data. The immediate eastward propagation was due to the easterly component of the initial velocity.